

Effects of Heterocyclic Aromatic Substituents on Binding Affinities at Two Distinct Sites of Somatostatin Receptors. Correlation with the Electrostatic Potential of the Substituents

Vidya Prasad,^{†,‡} Elizabeth T. Birzin,^{||} Cheryl T. McVaugh,[†] Rachel D. van Rijn,^{†,§} Susan P. Rohrer,^{*,||} Gary Chicchi,^{||} Dennis J. Underwood,^{*,⊥} Edward R. Thornton,^{*,†} Amos B. Smith, III,^{*,†} and Ralph Hirschmann^{*,†}

Department of Chemistry, University of Pennsylvania, Philadelphia, Pennsylvania 19104, Merck Research Laboratories, Rahway, New Jersey 07065, and DuPont Pharmaceutical Company, Wilmington, Delaware 19880

Received November 8, 2002

In our continuing program exploring glucose-based peptidomimetics of somatostatin (SRIF-14), we sought to improve the water solubility of our glycosides. This led to insights into the nature of the ligand binding sites at the SRIF receptor. Replacement of the C4 benzyl substituent in glucoside (+)-**2** with pyridinylmethyl or pyrazin-2-ylmethyl congeners increased water solubility and enhanced affinity for the human SRIF subtype receptor 4 (sst4). We attribute this effect to hydrogen bond formation. The pyridin-3-ylmethyl substituent at C4, when combined with the imidazol-4-ylmethyl group at C2, generated (–)-**19**, which has the highest affinity of a glucose-based peptidomimetic at a human SRIF receptor to date (K_i 53 ± 23 nM, $n = 6$ at sst4). The C4 heterocyclic congeners of glucosides bearing a 1-methoxy substituent rather than an indole side chain at the anomeric carbon, such as (+)-**16**, also provided information about the Trp⁸ binding pocket. We correlated the SARs at both the C4 and the Trp⁸ binding pockets with calculations of the electrostatic potentials of the diverse C4 aromatic substituents using Spartan 3-21G^(*) MO analysis. These calculations provide an approximate analysis of a molecule's ability to interact within a receptor binding site. Our binding studies show that benzene and indole rings, but not pyridinylmethyl nor pyrazin-2-ylmethyl rings, can bind the hydrophobic Trp⁸ binding pocket of sst4. The Spartan 3-21G^(*) MO analysis reveals significant negative electrostatic potential in the region of the π -clouds for the benzene and indole rings but not for the pyridinylmethyl or pyrazin-2-ylmethyl congeners. Our data further demonstrate that the replacement of benzene or indole side chains by heterocyclic aromatic rings typified by pyridine and pyrazine not only enhances water solubility and hydrogen bonding capacity as expected, but can also profoundly diminish the ability of the π -cloud of the aromatic substituent to interact with side chains of an aromatic binding pocket such as that for Trp⁸ of SRIF-14. Conversely, these calculations accommodate the experimental findings that pyrazin-2-ylmethyl and pyridinylmethyl substituents at C4- of C1-indole-substituted glycosides afford higher affinities at sst4 than the C4-benzyl group of (+)-**2**. This result is consistent with the high electron density in the plane of the heterocycle depicted in Figure 6 which can accept hydrogen bonds from the C4 binding pocket of the receptor. Unexpectedly, we found that the 2-fluoropyridin-5-ylmethyl analogue (+)-**14** more closely resembles the binding affinity of (+)-**8** than that of (+)-**2**, thus suggesting that (+)-**14** represents a rare example of a carbon linked fluorine atom acting as a hydrogen bond acceptor. We attribute this result to the ability of the proton to bind the nitrogen and fluorine atoms simultaneously in a bifurcated arrangement. At the NK1 receptor of substance P (SP), the free hydroxyl at C4 optimizes affinity.

Introduction

In 1987 we initiated studies to test the proposition that nonpeptidic mimetics of β -turns can be generated via the attachment of appropriate side chains to monosaccharide scaffolds typified first by glucose¹ and later by mannose.² The minimal pharmacophoric requirement

for the binding of peptides to all somatostatin (SRIF) receptor subtypes is the presence of adjacent indole and alkylamine side chains in the $i+1$ and $i+2$ positions of β -turns as in the tetradecapeptide SRIF-14, its crystalline congener octreotide and in **1** (Figure 1). The glycosides (+)-**2** and (–)-**3** designed to mimic this structural feature did indeed bind SRIF receptors on AtT-20 cells, albeit weakly (K_i ca. 15 μ M) (see Figure 1 for structures); a glycoside mimic (–)-**3** was found to be an SRIF agonist.^{1a,b} Later (+)-**2** and (–)-**3** were found to bind also human SRIF receptor subtypes, displaying the highest affinity at subtype 4 (sst4).² The SAR of (–)-**3** strikingly resembles that of the cyclic hexapeptide **1**.^{1a} For example, replacement of the axial Phe⁷ of SRIF-

* Corresponding author: R. Hirschmann, Department of Chemistry, University of Pennsylvania, 231 South 34th St., Philadelphia, PA 19104-6323. Phone: (215) 898-7398. Fax: (215) 573-9711. E-mail: rfh@sas.upenn.edu.

[†] University of Pennsylvania.

[‡] Present address: Gilead Sciences, 333 Lakeside Dr., Foster City, CA 94404.

^{||} Merck Research Laboratories.

[§] Present address: N.V. Organon, P.O. Box 20, The Netherlands.

[⊥] Bristol-Myers Squibb Co. (formerly DuPont Pharmaceutical Co.).

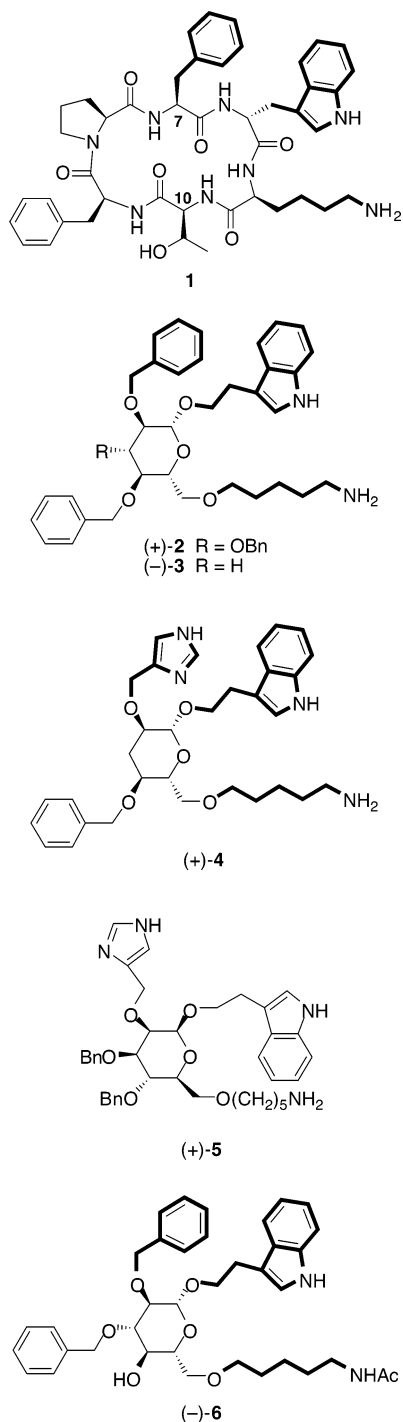


Figure 1. Potent SRIF agonist **1** and previously reported monosaccharide-based mimetics (+)-**2** and (-)-**3**. Congener (+)-**4** binds sst4, but not the NK1 receptor. Conversely, the 4-unsubstituted glucoside (-)-**6** is a potent substance P receptor ligand, but does not bind sst4. Analogues (+)-**2** and (-)-**3** bind both receptors. The L-mannose analogue (+)-**5** has a K_i of 100 nM at sst4,² an affinity enhancement by more than a factor of 15 over that of (+)-**2**.

14 or the Phe⁷ of **1** (SRIF-14 numbering) by His⁷ was known to enhance potency.³ We observed a corresponding affinity enhancement when the 2-benzyl side chain of (-)-**3** is replaced by the imidazol-4-ylmethyl moiety (+)-**4**.^{1a,2} Subsequently we achieved a K_i of 100 nM at sst4 with the congener (+)-**5**.² The underlying rationale (that the β -turn of **1**, defined by Trp⁸ and Lys⁹ (SRIF-14 numbering), is mimicked by the side chains of (+)-**2**

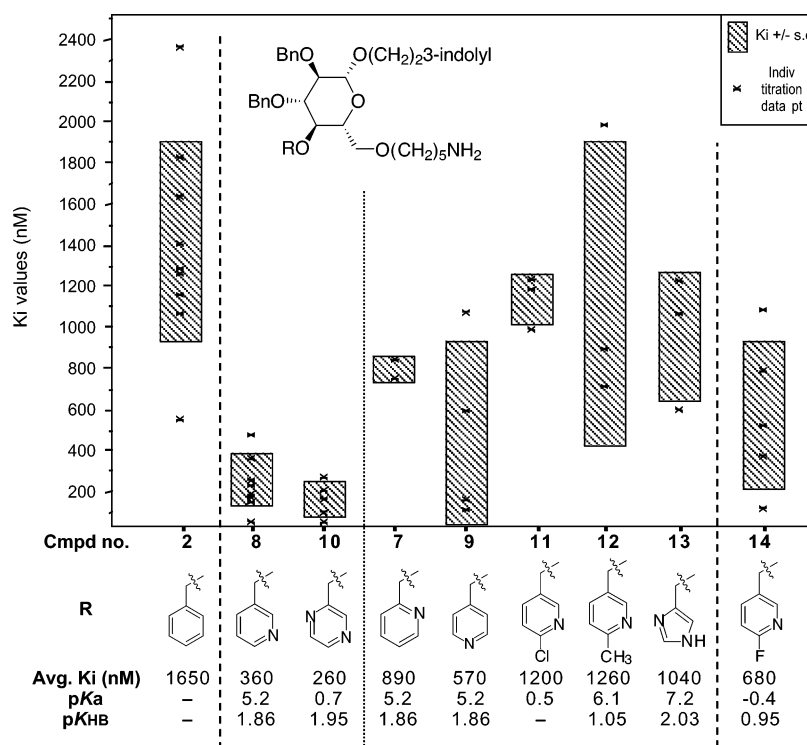
and (-)-**3** at C1 and C6) is supported by the parallelism in SARs between the peptide **1** and the glycoside (-)-**3**.^{1a} Thus, the Trp⁸ and Lys⁹ side chains of SRIF-14, of **1**, like their mimics in (+)-**2** and (-)-**3**, anchor these ligands to SRIF receptors. On the other hand, the receptor subtype profile—which depends on other side chains of the ligands, perhaps even their scaffolds and on other regions of the binding domain of the receptors—differs between SRIF-14, octreotide, and the c-hexapeptides, as well as the glycosides.^{4,5}

Unexpectedly, (+)-**2** was also found to bind the NK1 receptor of substance P (SP) as an antagonist, with a K_i of 150 nM.^{1c} Compound (-)-**6**, lacking a C4 benzyl substituent, has a K_i of 27 nM² at the NK1 receptor, but does not bind sst4, and the corresponding free amine has a comparable affinity (K_i 66 nM) at the NK1 receptor.⁶ Conversely, (+)-**4** binds sst4,² but not the NK1 receptor.⁶ Taken together these results show that we have synthesized analogues of (+)-**2** which are selective for either SRIF or NK1 receptors.

Structure–Activity Relationships (SARs) of C4 Heterocyclic Substituents. (a) At the NK1 Receptor. Herein we report the syntheses of the three isomeric C4 pyridinylmethyl congeners (+)-**7**, (+)-**8**, and (+)-**9** as well as other heterocyclic substituents that replace the 4-benzyl group of (+)-**2** (see Table 1 for structures). Binding affinities at the NK1 receptor were generally enhanced relative to (+)-**2**, but not significantly.^{7,8,9} Representative results are given in the Supporting Information. The high affinity of (-)-**6** (Figure 1) at the NK1 receptor implies that aromatic C4 substituents, even water soluble ones, such as the C4 pyridinylmethyl isomers, generate a less favorable interaction with this receptor. It is also possible that the C4 hydroxyl generates a favorable interaction with the NK1 receptor. Affinities were generally greater for the *N*-acetyl derivatives of the primary amines (not shown) than for the free amines at the NK1 receptor; the differences between diverse C4 heterocyclic substituents were small.

(b) Hydrogen-Bond Mediated Affinity Enhancement at sst4 via C4 Pyridinylmethyl or Pyrazin-2-ylmethyl Substitution. The SARs of the above-mentioned heterocyclic congeners at sst4 (see Table 1) differ markedly from those at the NK1 receptor. The pyridin-3-ylmethyl derivative (+)-**8** and especially the pyrazin-2-ylmethyl congener (+)-**10** displayed significantly enhanced affinities relative to (+)-**2** at sst4. The isomeric pyridinylmethyl congeners (+)-**7** and (+)-**9** also produced affinity enhancement, but to a lesser degree.

The Basis For Affinity Enhancement. The 5-fold affinity enhancement at sst4 of the neutral C4 pyrazin-2-ylmethyl analogue (+)-**10** over the 4-benzyl congener (+)-**2** is too small to be attributed to salt bridge formation between this heterocycle and the receptor. Directional hydrogen bond formation appears the most plausible explanation for the affinity enhancement of (+)-**10** as well as that of (+)-**7**, (+)-**8**, and (+)-**9**. The affinity enhancement is greatest for (+)-**8** and (+)-**10**, less so for (+)-**9**, and least for (+)-**7**; these results are also consistent with the directional nature of hydrogen bonds.¹⁰ We also considered an alternate explanation for the enhanced affinity of (+)-**8** and (+)-**10** over that of (+)-**2**: the C4 heterocyclic aromatic rings might act

Table 1. SARs of C4 Heterocycle-Containing Analogues at the sst4 Receptor of SRIF

^a pKa values are for the NH⁺ protonated heterocycles. PKHB values represent hydrogen bond basicity of the heterocycles (pyridine, etc.), obtained by FTIR spectrometry.¹⁴ All data points are shown; the center of the gray area represents the calculated K_i and the box graph depicts the standard deviation.⁶⁵ Data points within the 90% confidence limits (Q-test) were retained in the calculation of average K_i whether they lie within the standard deviation area (gray zone).⁶⁵ (For optical rotation signs of the compounds cited, see text.)

as facial π electron donors in edge-to-face aromatic–aromatic interactions within the C4 binding pocket.¹¹ The computed electrostatic potential surfaces, however, are inconsistent with this explanation (see below).

The ortho-substituted pyridinylmethyls (+)-**11** and (+)-**12** both had binding affinities comparable to that of (+)-**2** despite the striking difference of the pKa's of these two heterocycles. These results suggest unfavorable steric effects from the isosteric chloro and methyl substituents. The inductive effect should favor the methyl substituent, but only to the extent that hydrogen bonding is still possible. The imidazole nitrogen of (+)-**13** is more basic than the nitrogen of (+)-**8**: the diminished affinity may therefore be due in part to greater solvation, causing the increased binding energy to be more than offset by the desolvation energy required for the compound to enter the transmembrane domain. The decrease in binding affinity might also be partially due to the change in ring size, therefore affecting the directional nature of the hydrogen bonding of the imidazole compared with pyrazin-2-ylmethyl or pyridin-3-ylmethyl.^{12,13} In addition, the data show that changes in pKa and in pKHB have different effects on binding affinities.¹⁴

Pyrazine has two types of proton-acceptor sites: the nitrogen lone pairs and the ring π -cloud. Hydrogen bonding occurs only with the former, via the lone pairs of a nitrogen, analogous to that of pyridine.¹⁵ The conserved directionality of hydrogen bonding involving both pyridine and pyrazine nitrogens is consistent with their similar binding affinities.¹⁶ Both the pyridine and pyrazine are presumed to be largely unprotonated in the receptor, and their affinity enhancements are

consistent with a hydrogen bond rather than a salt-bridge.^{10,17} Steiner and Koellner indicate that the energies of hydrogen bonds cover a wide range (0.5 to over 30 kcal/mol).^{18,19} We conclude that hydrogen bonding capabilities, rather than the pKa values are consistent with the SARs.¹⁴

Showing that the pyridinylmethyl and pyrazin-2-ylmethyl congeners (+)-**7**, (+)-**8**, (+)-**9**, and (+)-**10** display higher binding affinities than the 4-benzyl analogue (+)-**2**, did not allow us to predict the effect of the fluorine substituent of (+)-**14**. The electronegativity of the fluorine atom should markedly reduce the presence of the lone electron pair around the nitrogen atom. Several investigators have examined the question whether a fluorine substituent attached to a carbon atom can act as a hydrogen bond acceptor, providing contradictory conclusions. These are briefly summarized below.

Dunitz and Taylor^{20,21} examined the crystal structures from the Cambridge Structural Database and the Brookhaven Protein Data Bank. They expressed the observed short H bond formation as a percentage of the opportunities for such H bonding and found this to be 42% for carbonyl oxygens, 32% for aryl amino nitrogens, but only 0.6% for carbon-linked fluorine atoms. Recent reports by Kool and co-workers²² are consistent with this analysis. Rozovsky, McDermott, and their co-workers reported crystallographic studies which revealed that fluorinated triosephosphate isomerase is indistinguishable from the wild type, and that the fluorine atom accepts a hydrogen bond from water and not from a protein residue.^{23,24} Barberich et al., however, provided examples for significant inter- and intramolecular hy-

drogen bonding between hydroxyl groups and C–F bonds, citing a H–F distance (2.01 Å) obtained by neutron diffraction, and an OH–F distance of 2.97 Å, obtained by X-ray diffraction.²⁵ The authors conclude that “many questions about the nature and strength of these dipole–dipole interactions and their biological importance remain unanswered.” Finally, Krueger and Mettee reported H bond formation constants (K_{assoc}) in CCl_4 solution at $\sim 28^\circ\text{C}$ with methanol of 1.5 for n-amyloxy fluoride and 0.11 for fluorobenzene.^{26,27}

In the event, the 2-fluoropyridin-5-ylmethyl derivative (+)-**14** (Table 1) displayed a K_i which more closely resembles that of the pyridin-3-ylmethyl congener (+)-**8** than that of the 4-benzyl analogue (+)-**2**. As mentioned above, the electronegativity of the fluorine atom makes it unlikely that the nitrogen atom of (+)-**14** per se can act as a hydrogen bond acceptor.²⁸ It is therefore of interest that anhydrous hydrogen fluoride is said to form nonlinear, zigzag hydrogen bonds, even in the gas phase,²⁹ supporting the proposition that fluorine can act as an hydrogen bond acceptor. This nonlinearity leads us to speculate that dipole interaction of the proposed hydrogen bond donor may involve *both* the pyridine nitrogen and the fluorine of (+)-**14**. Such nonlinearity might allow for a bifurcated hydrogen bond in which the proton is simultaneously bound to both the pyridine nitrogen and to the fluorine atom of (+)-**14**. Bifurcated arrangements have been observed in several crystal structures involving organic fluorine as a hydrogen bond acceptor.^{30,31} There is one reported case of three-center, bifurcated hydrogen bonding, in ammonium fluoroacetate.³²

Probing the Binding Mode of Pyridin-3-ylmethyl Analogue (+)-8. We previously showed that the 1-methoxyglycoside (+)-**15**, which lacks the Trp⁸ mimicking C1 indole substituent, binds SRIF receptors via an alternate binding mode,² made possible by the radial symmetry of the glucose as^{7–9} depicted in Figure 2b. This raised the interesting question whether the C1 indole containing C4 pyridinylmethyl and pyrazin-2-ylmethyl analogues show enhanced affinity over the C4-benzyl congener *because* they, too, bind via this alternative binding mode as implied by part e in Figure 2 (i.e., the pyridinylmethyl/pyrazin-2-ylmethyl rings serve as improved indole surrogates). We therefore synthesized the C1-methoxy pyridinylmethyl analogues (+)-**16a** through (+)-**16c** as well as the C1-methoxy pyrazin-2-ylmethyl congener (+)-**17** and 2-fluoropyridin-5-ylmethyl congener (+)-**18** (see Figure 3). None of these congeners bind sst4 at concentrations of $10\ \mu\text{M}$. We therefore conclude that (+)-**8** and, by analogy, (+)-**10** bind as shown in Figure 2c and not as shown in Figure 2e.

Relationship between the C4 Substituent of (+)-2 and Peptidal SRIF Receptor Ligands. Molecular modeling reveals³³ that the Trp⁸ and Lys⁹ side chains, the functionalities of SRIF-14 that are essential for binding, overlay well with the corresponding side chains of octreotide, the only crystalline peptidal or glycosidic SRIF receptor ligand.³⁴ This is reassuring because these and the related side chains of (+)-**2** and of (–)-**3** fit this same pocket in the receptor. It is possible that Thr¹⁰ and Thr¹² of SRIF map to the same positions as does the C4-benzyl of the sugar (see Figure 4). It is known that the Thr¹⁰ side chain is not required for

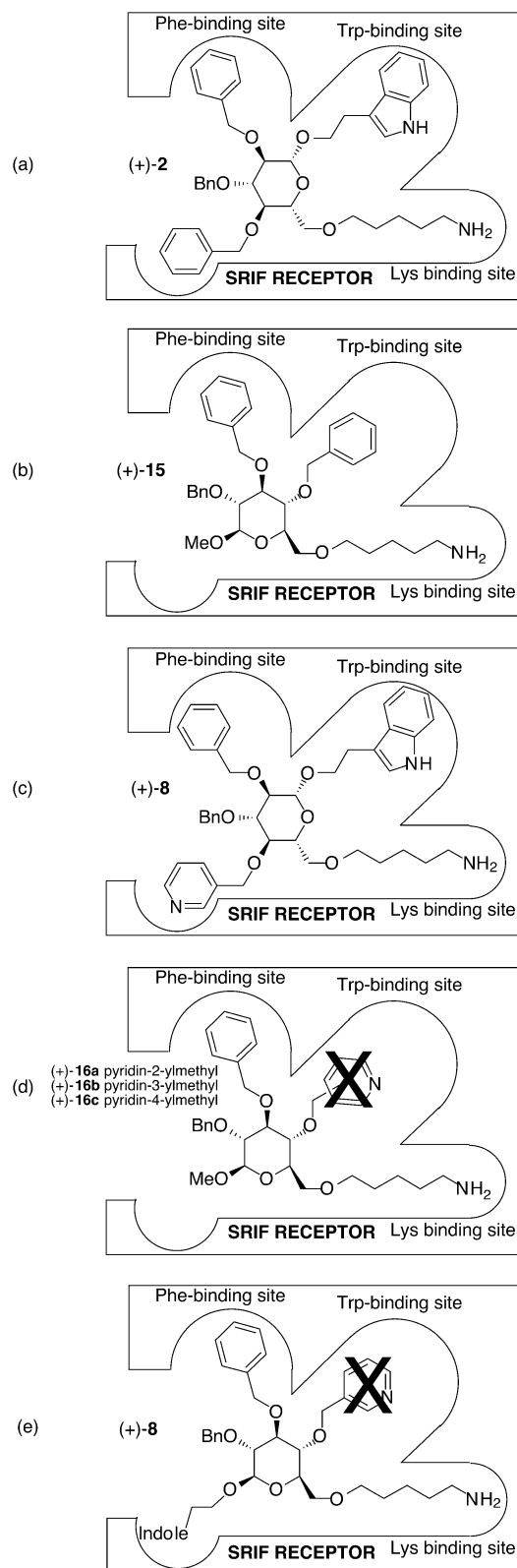


Figure 2. Probing the binding mode for pyridinylmethyl glycosides at sst4. Presentations d and e are inconsistent with the data. (a) Binding mode of (+)-**2**. (b) The established binding mode for ligand (+)-**15**, lacking an indole side chain.² (c) The binding mode proposed herein for the pyridin-3-ylmethyl-substituted analogue (+)-**8**. (d) Congeners of (+)-**15** with a C4 heterocyclic substituent do not bind. (e) Conclusion: the alternate binding mode typified by (+)-**15** does not apply to (+)-**8**, and therefore the pyridinylmethyl and the pyrazin-2-ylmethyl substituents do not serve as indole replacements.

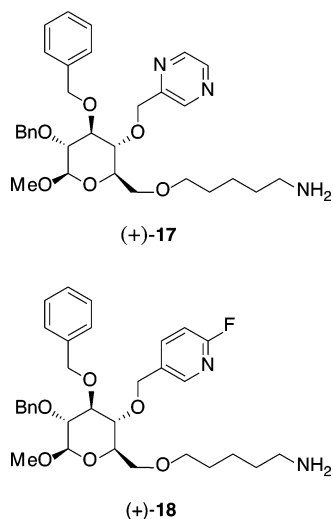


Figure 3. Pyrazinyl- and 2-fluoropyridin-5-ylmethyl-containing methyl glycosides (+)-17 and (+)-18.

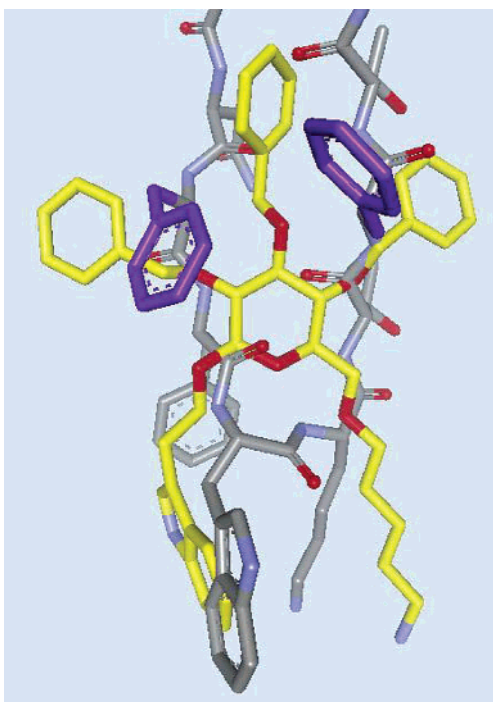


Figure 4. Comparison of SRIF-14 and a sugar (+)-2 (yellow carbons). This alignment reveals the overlap of the two essential side chains (Trp⁸ and Lys⁹) of SRIF-14 and their mimics in the glucoside. Phe⁶ and Phe¹¹ of SRIF-14, which are thought to stabilize its bioactive conformation, are shown in purple. The figure also reveals that the C4-benzyl of the sugar is positioned close to the Thr¹⁰/Thr¹² side chains of SRIF-14, but it is also close to Phe¹¹.

binding, since Gly¹⁰-containing peptides are highly potent.³⁵ Moreover, the C4-benzyl group of (+)-2 also overlaps well with the C-terminal threoninol of octreotide (see Figure 5). These observations suggest a hydrophilic environment for the C4 region of the glucoside. Nevertheless, the large structural differences between the glycoside and the peptidal ligands, and even between SRIF-14 and octreotide, do not allow us to eliminate the possibility that the C4 position of the sugar more closely overlaps Phe¹¹ of SRIF. This issue is further complicated by the fact that Phe⁶ and Phe¹¹

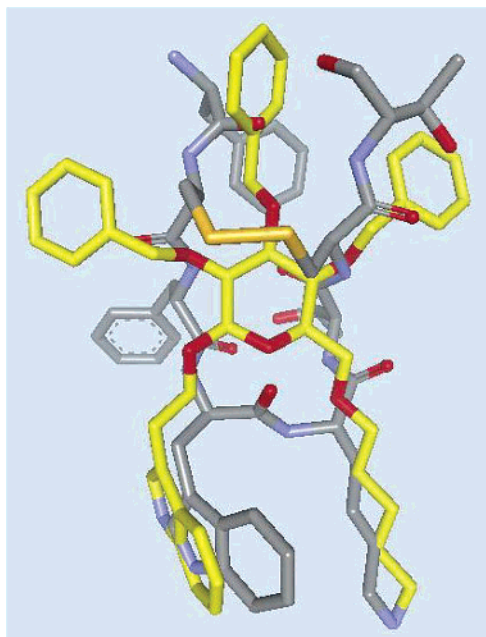


Figure 5. A stereo representation of the averaged NMR structural data of octreotide and of a representative sugar (+)-2. There is no equivalent for Phe¹¹ of SRIF-14 in octreotide, which, however, has a counterpart for the C3-benzyl of the sugar. Interestingly, the C-terminal residue of octreotide (threoninol) overlaps the C4-benzyl of the sugar.

of SRIF-14 have been shown to stabilize the bioactive conformation of this peptide via a herringbone-type interaction.³⁶ Nevertheless our binding data for the C4 heterocycles allow us to conclude that sst4 tolerates hydrophilic aromatic groups at the C4 position of the sugar.³⁷

Why Do the C1-Methoxy-C4-heterocycles Fail To Bind sst4? Compounds (+)-16a–c (Figure 2) and (+)-17 and (+)-18 (Figure 3), all of which are congeners of the ligand (+)-15, fail to bind sst4. This indicates that the C4 heterocycles, unlike the C4-benzyl, cannot be accommodated in the Trp⁸ binding pocket (Figure 2). We considered two possible explanations:

(1) An Unfavorable Desolvation Requirement? If the C4 heterocyclic substituents are solvated, the energy required for desolvation might interfere with binding in the Trp⁸ binding pocket. We therefore computed the electrostatic partial charges on the NH of indole and piperidine and found them to be identical (+0.37 and +0.36, respectively). This suggests that the desolvation energies of the indole and the piperidine NH's would not differ significantly. Since Trp binds the Trp⁸ binding pocket by definition, we reject this interpretation, preferring the rationalization discussed below.

(2) The Importance of the π -Clouds of Aromatic rings for Binding of the Trp⁸ Receptor Pocket. **Application of Spartan 3-21G^(*) MO Analysis.** Figure 6 shows the calculations of aromatic electrostatic potentials via Spartan 3-21G MO^(*) analysis. It reveals that the benzene or indole rings unlike the pyridine or pyrazine rings found in (+)-16 through (+)-18 (Figures 3 and 4) can provide for effective π -donor interactions with, for example, an edge of an aromatic amino acid in the Trp⁸ binding pocket. Aromatic–aromatic interactions make an important contribution to nonbonded

binding potential and play a significant role in protein stabilization (0.6–1.3 kcal/mol).³⁸ Hunter et al.¹¹ have proposed a model for aromatic interactions.^{39–42}

Both the pyridine and pyrazine heterocycles have electron deficient π -systems and differ from the relatively electron-rich π -systems of the indole and the benzene rings. If such electron-rich π systems are important for binding in the Trp⁸ binding pocket of the sst4 receptor, this difference would explain the observed loss of binding of analogues (+)-**16a–c** through (+)-**18**. Ab initio calculations by Samanta et al.,⁴³ on the other hand, suggested that the interaction energies with the π -face are of comparable magnitude for benzene and pyridine although there is a greater variation over the pyridine ring, thus making certain orientations more stabilizing than others. Our data are consistent with the views of Cozzi et al.⁴¹ and of Doyan and Jain⁴² as detailed below.

Spartan 3-21G(*) Molecular Orbital Analysis of Aromatic Electrostatic Potentials. We computed the electrostatic potentials of the relevant aromatic substituents at C4 of the glycosides, using Spartan 3-21G(*) molecular orbital analysis.⁴⁴ The electrostatic potential is defined as the energy of interaction of a point positive charge with the nuclei and the electrons of the molecule of interest. The potentials for the benzene, pyridine, 2-fluoropyridine, pyrazine, and indole rings are shown in Figure 6. The Spartan 3-21G(*) molecular modeling

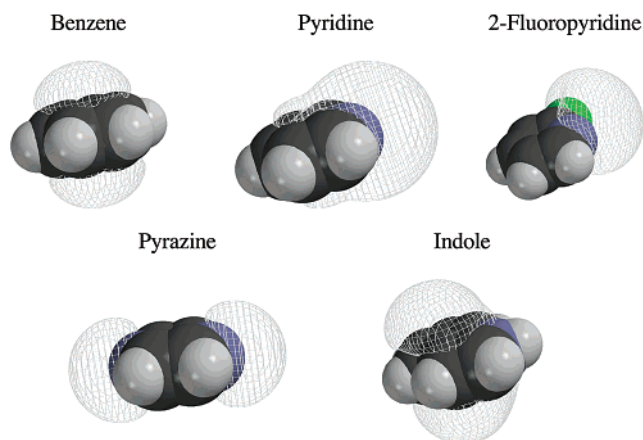


Figure 6. Spartan 3-21G(*) MO analysis of aromatic electrostatic potentials which involve interactions of a positive charge not only with the π -cloud but also with all other electrons and nuclei of the molecule. The mesh surfaces depicted are the surfaces upon which the electrostatic potential (i.e., the attraction of the molecule for a positive point charge) equals -10 kcal mol⁻¹.

analysis explains why in the case of the glycosides containing the C1 indole substituent, typified by (+)-**2**, the C4 heterocyclic aromatics (+)-**7** through (+)-**10** and (+)-**14** reveal enhanced affinities compared with (+)-**2**. Hydrogen bonding of the unshared electron pairs of the C4 heterocyclic ring with a presumed hydrogen bond donor of an amino acid in the binding pocket offers the best explanation for the affinity enhancement.

The measurement of the electrostatic potential surfaces (Figure 6) convincingly argues against an alternate explanation, that the C4 heterocyclic aromatic rings act as facial π -electron donors in edge-to-face aromatic–aromatic interactions within the C4 binding pocket.

Significantly, the electron distributions of the heterocyclic aromatics at C4 also explain why the C1-methoxy-C4-heterocyclics typified by (+)-**16**, lacking a significant negative potential in the region of the π -cloud, fail to bind the aromatic Trp⁸ binding pocket.

Models generated of the interaction of SRIF with receptor subtypes 1 and 2 by Kaupmann et al.⁴⁵ suggest that Trp⁸ of SRIF binds in an aromatic cavity involving the residues Phe²³², Trp²⁸⁴, and Tyr²⁸⁸. In addition, they provided a sequence alignment for all receptor subtypes which allows one to conclude that in the Trp⁸ binding pocket, Phe²³² (human sst1 numbering) and Trp²⁸⁴ are conserved among the five human receptor subtypes and Tyr²⁸⁸ is conserved among sst1–4 (but is replaced by Phe at sst5). We conclude that the Trp⁸ binding pocket requires a ligand that contains electron-rich π -clouds. This is not the case in the C4 binding pocket where a hydrogen bond donor increases binding with the heterocyclic substituents of (+)-**7** through (+)-**10** and (+)-**14**.

Further Improvement in Affinity. Replacement of Phe⁷ by His⁷ in both SRIF-14 and in the cyclic hexapeptide **1**⁴⁶ enhances affinity. In the sugar series, replacement of the C2 benzyl of (–)-**3** by the corresponding imidazol-4-ylmethyl similarly led to comparable enhancement in affinity.^{1a} To test further the presumption (Figure 2c) that the pyridin-3-ylmethylindole-containing sugar binds the receptor via the C1 indole- and the C6 lysine-mimicking side chains, we introduced a imidazol-4-ylmethyl side chain at C2 to afford (–)-**19** (Figure 7).

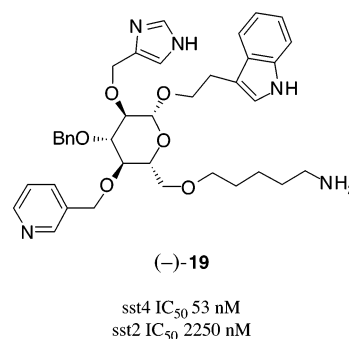
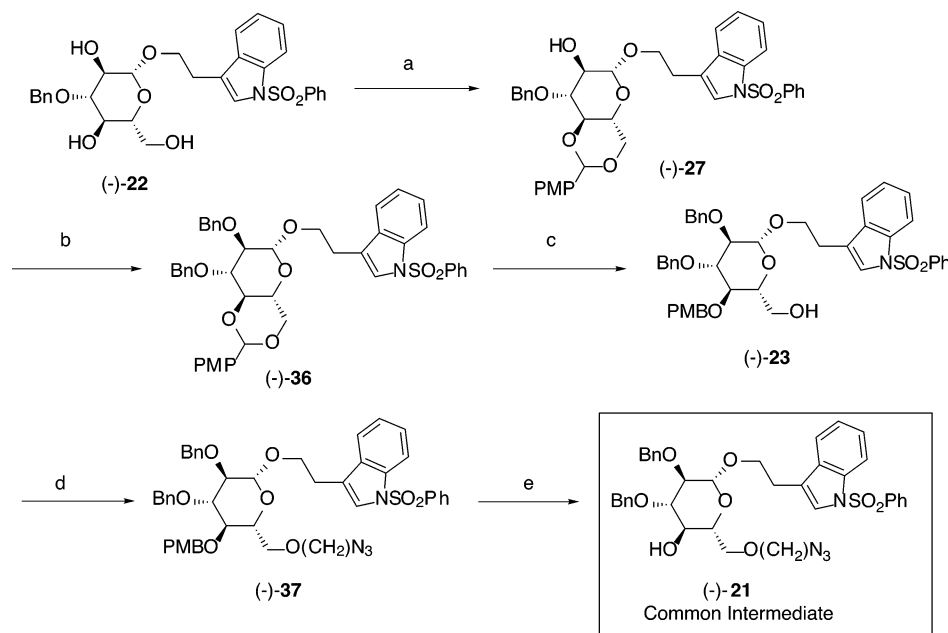


Figure 7. Incorporating a imidazol-4-ylmethyl at C2 of a C4 pyridin-3ylmethyl ligand; enhanced binding affinity at sst2 and sst4.

This congener indeed showed a further enhancement in affinity (sst4 K_i 53 ± 23 nM, $n = 6$) providing a 31-fold affinity enhancement over (+)-**2** while retaining specificity for sst4.

Prior to the synthesis of (–)-**19**, our highest affinity ligand for sst4 was the diastereomeric L-mannose derivative (+)-**5** (K_i 100 nM)² which displays the C2 substituent in an axial disposition, resembling Phe⁷ of SRIF in this regard.⁴⁷ Hoping to increase affinity further, we replaced the C4 benzyl substituent of (+)-**5** by the pyridin-3-ylmethyl congener, affording (+)-**20**; we were disappointed that this chemically challenging synthesis was found to diminish affinity (K_i 800 nM, see Figure 8).

Exploratory Pharmacokinetic Studies. Representative substituted glycosides were subjected to hydrolysis conditions with both gastric acid and glucosidases and were found to be stable.⁴⁸ These results,

Scheme 1. Synthesis of Common Intermediate (–)-21^a

^a Reagents: (a) *p*-methoxybenzaldehyde dimethyl acetal, *p*TSA, CHCl₃; (b) BnBr, NaH, TBAI, THF; (c) DiBAL-H, CH₂Cl₂; (d) NaH, TfO(CH₂)₅N₃, THF; (e) DDQ, CH₂Cl₂:H₂O (20:1).

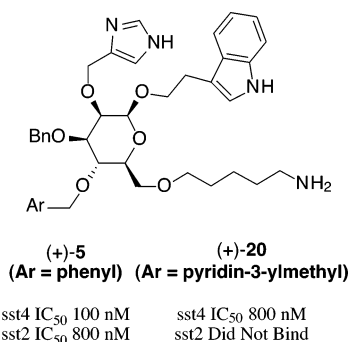
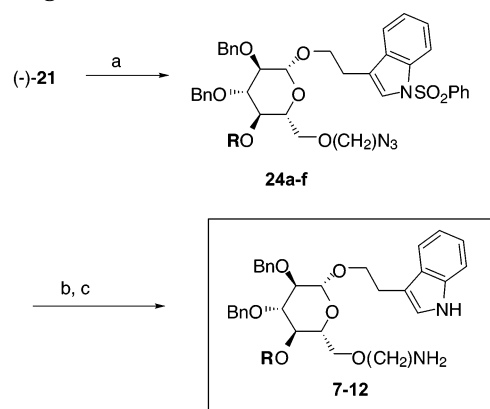


Figure 8. Binding affinities of imidazole-containing L-mannosides. (+)-5 reveals the affinity-enhancing effect of the imidazol-4-ylmethyl. In (+)-20 an unfavorable interaction apparently results from the presence of both the equatorial pyridin-3-ylmethyl and the axial imidazol-4-ylmethyl side chains.

together with those reported by others,^{49,50} demonstrate the stability of substituted glycosides to both enzymatic and gastric acid hydrolysis. The calculated logP of (–)-19 (clogP 5.35) is significantly lower than that of our first designed mimetic (+)-2 (clogP 9.14).⁵¹ Indeed, (–)-19 displays improved aqueous solubility, which allowed us to assess bioavailability via parenteral administration. Not surprisingly, (–)-19 was extensively metabolized by the cytochrome P-450 superfamily of isozymes.⁵² We are, therefore, exploring the reduction in the number of aromatic side chains⁵³ in order to identify and block potential oxidation sites.⁵⁴ The use of carbohydrates as orally available therapeutics has been preceded.^{55,56}

Chemistry. Preparation of analogues (+)-7 through (+)-14, containing a C1 indole substituent, all began with the alcohol (–)-21.⁵⁷ This alcohol was prepared in five steps from known triol (–)-22 as shown in Scheme 1.² Subsequent alkylation of (–)-21 in a THF:DMF (4:1) mixed solvent system with 2-picolyl, 3-picolyl or 4-picolyl chloride isomers afforded analogues 24a–c, respectively, in moderate yields (Scheme 2). The mixed

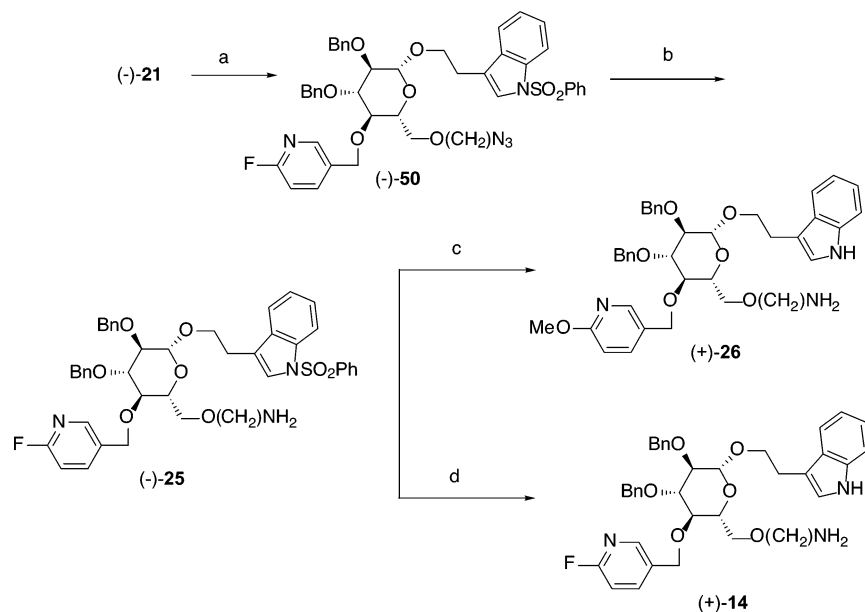
Scheme 2. Synthesis of C4 Heterocycle-Substituted Analogues^a

R = pyridin-2-ylmethyl, pyridin-3-ylmethyl, pyridin-4-ylmethyl, pyrazin-2-ylmethyl, 2-chloropyridin-5-ylmethyl, 2-methylpyridin-5-ylmethyl

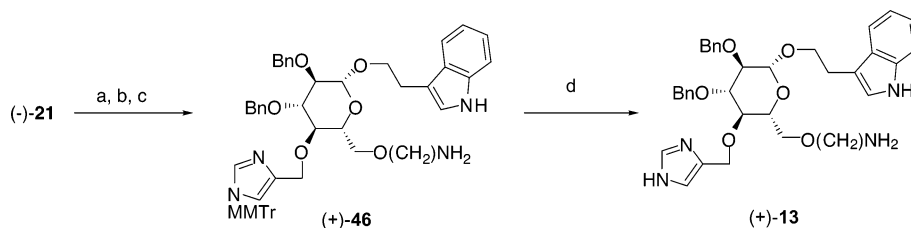
^a Reagents: (a) NaH, R-Cl, TBAI, THF:DMF (4:1); (b) PPh₃, THF, H₂O; (c) NaOH, MeOH.

solvent system was required since the pyridinylmethyl chlorides, obtained as their hydrochloride salts, were only slightly soluble in THF. Attempts to obtain the free pyridinylmethyl chlorides or to use pyridinylmethyl triflates resulted only in polymerization. We attribute the moderate yields to the low reactivity of the pyridinylmethyl chloride electrophiles and to the instability of the phenyl sulfonamide in the presence of strong alkali base, particularly in the ion-stabilizing solvent DMF. Introduction of the pyrazin-2-ylmethyl,⁵⁸ 2-chloropyridin-5-ylmethyl, and 2-methylpyridin-5-ylmethyl groups also provided the desired products (24d–f, respectively).

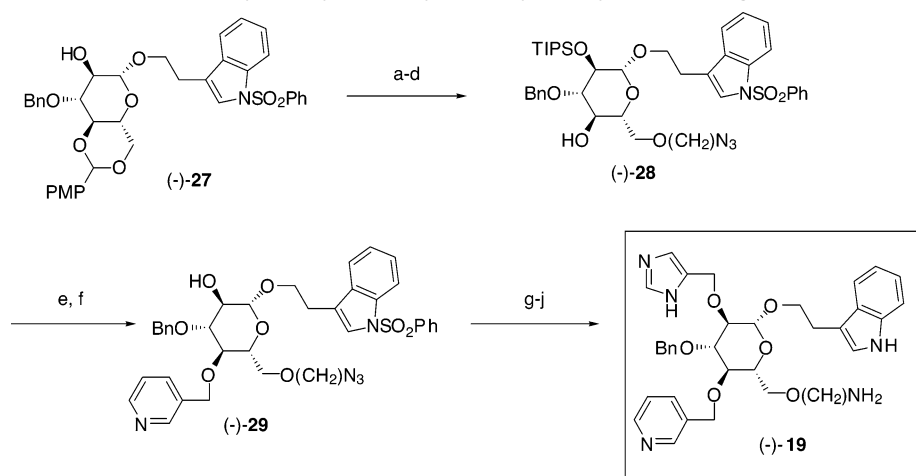
Staudinger reduction^{59,60} of the azides then gave the corresponding amines in good yield. Removal of the sulfone moiety by basic hydrolysis completed construction of the analogues (+)-7 through (+)-12, all containing a C4 heterocyclic substituent.

Scheme 3. Synthesis of the 2-Fluoropyridin-5-ylmethyl Analogue^a

^a Reagents: (a) NaH, 5-chloromethyl-2-fluoropyridine, TBAI, THF; (b) PPh₃, THF, H₂O; (c) NaOH, MeOH; (d) KOH, MeCN.

Scheme 4. Synthesis of Imidazole-Bearing Analogue (+)-13^a

^a Reagents: (a) NaH, MMTr-protected 4-chloromethylimidazole, TBAI, THF:DMF (4:1); (b) PPh₃, THF, H₂O; (c) NaOH, MeOH; (d) TFA, CH₂Cl₂.

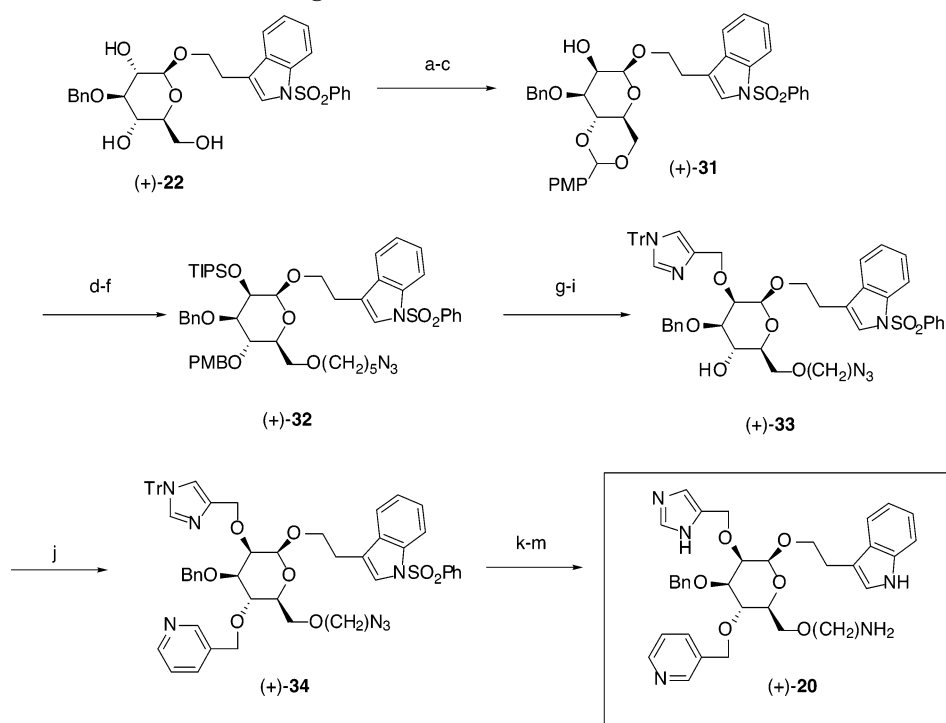
Scheme 5. Synthesis of an Imidazol-4-ylmethyl- and Pyridin-3-ylmethyl-Containing D-Glucoside^a

^a Reagents: (a) TIPSOTf, 2,6-lutidine; (b) DiBAL-H, CH₂Cl₂; (c) NaH, TfO(CH₂)₅N₃, THF; (d) DDQ, CH₂Cl₂:H₂O (20:1); (e) NaH, 3-pyridinylmethyl chloride, TBAI, THF:DMF (4:1); (f) TBAF, THF; (g) NaH, MMTr-protected 4-chloromethylimidazole, TBAI, THF:DMF (4:1); (h) PPh₃, THF, H₂O; (i) NaOH, MeOH; (j) TFA, HS(CH₂)₂SH, CH₂Cl₂.

Synthesis of the 2-fluoropyridin-5-ylmethyl analogue (+)-14 (Scheme 3) required modification of the procedure for the removal of the indole protecting group. Treatment of (-)-21 with NaH in THF followed by 5-chloromethyl-2-fluoropyridine provided the C4-alkylated product. The azide was then reduced to furnish amine (-)-25. Subsequent treatment of (-)-25 with methanolic NaOH removed the indole protecting group

and also displaced the fluorine on the pyridyl ring to generate the 2-methoxypyridin-5-ylmethyl analogue (+)-26. On the other hand, treatment with 8 N KOH in acetonitrile afforded the desired 2-fluoropyridin-5-ylmethyl (+)-14, albeit in low yield.

The synthesis of the imidazole-bearing analogue (+)-13 (Scheme 4) began with alkylation of (-)-21 employing *N*-monomethoxytrityl (MMTr)-protected 4-chloromethyl

Scheme 6. Synthesis of L-Mannoside Analogue (+)-**20**^a

^a Reagents: (a) *p*-methoxybenzaldehyde dimethyl acetal, CSA, CHCl₃; (b) Ac₂O, DMSO; (c) L-selectride, THF; (d) TIPSOTf, 2,6-lutidine, CH₂Cl₂; (e) DiBAL-H, CH₂Cl₂; (f) TfO(CH₂)₅N₃; (g) TBAF, THF; (h) NaH, Tr-protected 4-chloromethylimidazole, TBAI, THF:DMF (4:1); (i) DDQ, CH₂Cl₂, pH 6 buffer; (j) NaH, 3-pyridinylmethyl chloride, TBAI, THF:DMF (4:1); (k) DTT, TEA, MeOH; (l) TFA, HS(CH₂)₂SH, CH₂Cl₂; (m) NaOH, EtOH.

imidazole⁶¹ in a THF:DMF mixed solvent. Unmasking of the azide again by Staudinger reduction,^{59,60} provided the amine in excellent yield. Basic solvolysis (NaOH, MeOH) at reflux accomplished removal of the indole protecting group; subsequent removal of the MMTr protecting group with TFA yielded the C4-imidazol-4-ylmethyl analogue (+)-**13**.

The synthesis of C2-imidazol-4-ylmethyl, C4-pyridin-3-ylmethyl β-D-glucose (–)-**19** was accomplished by first introducing the pyridinylmethyl substituent at C4, followed by the more labile imidazol-4-ylmethyl substituent at C2. The previously prepared *p*-methoxybenzylidene alcohol (–)-**27** (Scheme 5) was protected at C2 by the triisopropylsilyl (TIPS) group; selective opening of the *p*-methoxybenzylidene acetal with DiBAL-H yielded the C6 primary alcohol. Subsequent treatment with NaH in diethyl ether followed by addition of the crude 5-azidopentyl triflate installed the azide precursor of the lysine side chain mimic. Oxidative-removal of the C4 *p*-methoxybenzyl group with DDQ yielded the C4 alcohol (–)-**28**, which upon etherification in a mixed solvent system [THF:DMF (4:1)] with 3-picoyl chloride and desilylation with tetrabutylammonium fluoride (TBAF) in THF furnished the C2 alcohol (–)-**29**. Subsequent alkylation with (*N*-MMTr)-4-chloromethylimidazole proceeded smoothly to afford the fully substituted glycoside (Scheme 5).

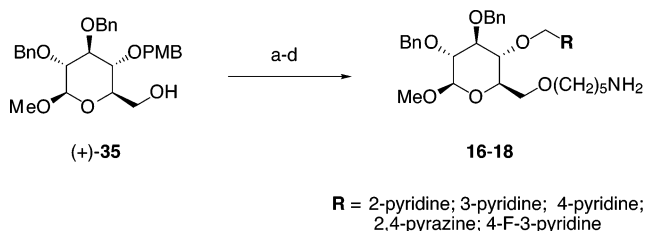
Three operations were then required to arrive at desired analogue (–)-**19**: (1) Staudinger reduction^{59,60} of the azide to afford the amine; (2) removal of the indole sulfonamide; and (3) acidic removal of the monomethoxytrityl moiety in the presence of ethane dithiol as a scavenger (67%, three steps).

The synthesis of the C2-imidazol-4-ylmethyl, C4-pyridin-3-ylmethyl β-L-mannose analogue (+)-**20** began

with (+)-**22** (Scheme 6), the enantiomer of the triol employed in Scheme 1. Conversion to the corresponding *p*-methoxybenzylidene acetal, followed by oxidation and reduction with L-selectride, afforded the axial alcohol (+)-**31**. Protection of the C2 alcohol as a TIPS-ether, selective opening of the *p*-methoxybenzylidene acetal with DiBAL-H, and alkylation of resultant C6 alcohol via acid-catalyzed etherification then furnished (+)-**32** in a 53% yield for the three steps. Removal of the axially oriented TIPS protecting group with TBAF proceeded in good yield. Etherification of the C2 alcohol with MMTr-protected 4-chloromethylimidazole⁶² then furnished the imidazole-bearing mannoside. Unfortunately treatment of the latter with DDQ resulted in complete removal of the MMTr protecting group of the imidazole, with only partial removal of the PMB protecting group. Thus, in this instance the MMTr protecting group proved to be too labile relative to the *p*-methoxybenzyl ether functionality.

To overcome this difficulty, the more robust trityl group was selected as the protecting group for the imidazole ring. Alkylation with trityl-protected 4-chloromethylimidazole (66%), followed by DDQ-mediated removal of PMB-protecting group at 0–5 °C in a pH 6.0 buffer, afforded alcohol (+)-**33**. Subsequent reaction of (+)-**33** with 3-picoyl chloride hydrochloride afforded the fully elaborated (+)-**34** in 76% yield. Staudinger reduction of azide (+)-**34** using triphenylphosphine afforded the desired amine, albeit in low yield. Unmasking of the amine with dithiothreitol⁶² in the presence of triethylamine, however, proceeded smoothly. Removal of the trityl protecting group under acidic conditions was then followed by deprotection of the indole to afford (+)-**20** in 71% yield (two steps).

Synthesis of methyl glucosides (+)-**16a–c**, (+)-**17**, and

Scheme 7. Synthesis of Various C4-Substituted Methyl Glycosides^a

^a Reagents: (a) NaH, THF, $\text{TfO}(\text{CH}_2)_5\text{N}_3$; (b) DDQ, CH_2Cl_2 ; H_2O (20:1); (c) NaH, $\text{R-CH}_2\text{Cl}$, TBAI, DMF; (d) PPh_3 , THF, H_2O .

(-)-**18** (Scheme 7) began with etherification of the known C6-alcohol (+)-**35**.⁶³ Oxidative removal of the *p*-methoxybenzyl group furnished the common C4-alcohol intermediate. Etherification with the appropriate picolyl or pyrazin-2-ylmethyl chlorides, followed by unmasking of the primary amine (Staudinger reduction) yielded analogues (+)-**16** through (+)-**18**.

Biological Methods. Binding assays at the human *sst4* receptor were performed using (3-¹²⁵I-Tyr¹¹)-SRIF-14 as the radioligand. The Packard Unifilter assay for SRIF subtype receptor binding was utilized for these experiments as described by Birzin and Rohrer.⁶⁴

Conclusion

Modifications to improve the water solubility of our glycosides provided us with insights into the nature of the ligand binding sites at both the NK1 and SRIF receptors. For the former we showed that the free C4 hydroxyl congener (-)-**6** provided optimal affinity (K_i 27 nM) since the C4 benzyl and even the three isomeric water-solubilizing C4 pyridinylmethyl analogues created less favorable interactions with the NK1 receptor.

On the other hand, at the SRIF receptor, the pyrazin-2-ylmethyl and the three isomeric C4 pyridinylmethyl substituents enhance affinity. The pyridin-3-ylmethyl congener (+)-**8** and the pyrazin-2-ylmethyl (+)-**10** proved most effective. We varied both the electronic and steric properties of the C4 substituent and concluded that affinity enhancement can be attributed to a directed hydrogen bond. The high affinity of the C4 pyrazin-2-ylmethyl congener, a neutral heterocyclic substituent, also suggests formation of a hydrogen bond. It is noteworthy that the fluoro-substituted pyridin-3-ylmethyl congener (+)-**14** (Table 1) can act as a hydrogen bond acceptor possibly because of the bifurcation that would allow the hydrogen bond to interact both with the nitrogen and the neighboring fluorine.

Introduction of a pyridinylmethyl group also improved aqueous solubility, facilitating pharmacokinetic studies and providing affinity enhancement specific for *sst4*. This substitution, when combined with the affinity enhancing imidazol-4-ylmethyl group at C2, generated a more water-soluble ligand (-)-**19** with a K_i of 53 nM. Through incorporation of the imidazol-4-ylmethyl affinity-enhancing substituent into the pyridin-3-ylmethyl-containing glycoside (-)-**19**, we were able to provide additional evidence that (+)-**8** binds in the same manner as other indole-containing ligands.

Finally, the incorporation of heterocyclic substituents into glycoside ligands proved to be a useful tool to probe the interaction of such ligands with noncrystalline transmembrane GPCRs. We found that a pyridinylm-

ethyl ring can replace a benzyl ring in the C4 position of indole-containing glucosides at the NK-1 and SRIF receptors but not in the Trp⁸ binding pocket of the SRIF receptor. These results are explained by our calculations of the electrostatic potentials of the diverse C4 substituents, showing that only the benzene ring, and not the pyridine and pyrazine congeners, display a π -electron cloud resembling that of the indole ring of SRIF-14, of **1**, and of (+)-**2**. Thus replacement of benzene or indole side chains by heterocyclic aromatic rings typified by pyridine and pyrazine produce two effects: they enhance water solubility and hydrogen bonding capacity as expected, but they also diminish the ability of the π -cloud associated with the heterocyclic ring to interact with side chains of an aromatic binding pocket such as that for Trp⁸ of SRIF-14.

Acknowledgment. Financial support was provided by the National Institutes of Health through Grant GM-41821. We also thank Merck Research Laboratories for an unrestricted grant. It is a pleasure to acknowledge the significant contribution of Dr. Maria Cichy-Knight who carried out our initial attempts to install the pyridinylmethyl side chains into the C3 and C4 positions of the glucoside. It is also satisfying to thank Dr. Margaret A. Cascieri for her profound contributions to our research prior to her recent career change. We thank Mr. Adam Charnley for proofreading this manuscript. The authors are also appreciative of Mr. Paul Marchesano for his expert assistance in the preparation of this manuscript. Finally, we thank the three referees for their valuable suggestions.

Supporting Information Available: Biological methods and binding data for the hNK1 receptor; experimental details of the hydrolytic stability studies; complete characterization of all analogues and synthetic intermediates, including ¹H NMR, ¹³C NMR, HRMS, optical rotation, and IR. This material is available free of charge via the Internet at <http://pubs.acs.org>.

References

- (1) (a) Hirschmann, R.; Nicolaou, K. C.; Pietranico, S.; Leahy, E. M.; Salvino, J.; Arison, B. H.; Cichy, M. A.; Spoons, P. G.; Shakespeare, W. C.; Sprengeler, P. A.; Hamley, P.; Smith, A. B., III; Reisine, T.; Raynor, K.; Maechler, L.; Donaldson, C.; Vale, W.; Freidinger, R. M.; Cascieri, M. A.; Strader, C. D. De-novo Design and Synthesis of Somatostatin Non-Peptide Peptidomimetics Utilizing β -D-Glucose as a Novel Scaffolding. *J. Am. Chem. Soc.* **1993**, *115*, 12550–12568. (b) Nicolaou, K. C.; Salvino, J. M.; Raynor, K.; Pietranico, S.; Reisine, T.; Freidinger, R. M.; Hirschmann, R. Design and Synthesis of a Peptidomimetic Employing β -D-Glucose for Scaffolding. In *Peptides – Chemistry, Structure, and Biology: Proceedings of the 11th American Peptide Symposium*; Rivier, J. E.; Marshall, G. R., Eds.; ESCOM: Leiden, 1990; pp 881–884. (c) Hirschmann, R.; Nicolaou, K. C.; Pietranico, S.; Salvino, J.; Leahy, E. M.; Sprengeler, P. A.; Furst, G.; Smith, A. B., III; Strader, C. D.; Cascieri, M. A.; Candelero, M. R.; Donaldson, C.; Vale, W.; Maechler, L. Non-peptidic Peptidomimetics with a β -D-Glucose Scaffolding. A Partial Somatostatin Agonist Bearing a Close Structural Relationship to a Potent, Selective Substance P Antagonist. *J. Am. Chem. Soc.* **1992**, *114*, 9217–9218.
- (2) Hirschmann, R.; Hynes, J., Jr.; Cichy-Knight, M. A.; van Rijn, R. D.; Sprengeler, P. A.; Spoons, P. G.; Shakespeare, W. C.; Pietranico-Cole, S.; Barbosa, J.; Liu, J.; Yao, W.; Rohrer, S.; Smith, A. B., III. Modulation of Receptor and Receptor Subtype Affinities Using Diastereomeric and Enantiomeric Monosaccharide Scaffolds as a Means to Structural and Biological Diversity. A New Route to Ether Synthesis. *J. Med. Chem.* **1998**, *41*, 1382–1391.
- (3) Nutt, R. F.; Colton, C.; Dylion; Veber, D. F.; Slater, E. L.; Saperstein, R. Somatostatin Analogues with Improved Oral Bioavailability. *Klin. Wochenschr.* **1986**, *64*, 71–73.

- (4) Hoyer, D.; Bell, G. I.; Berelowitz, M.; Epelbaum, J.; Feniuk, W.; Humphrey, P. P. A.; O'Carroll, A.-M.; Patel, Y. C.; Schonbrunn, A.; Taylor, J. E.; Reisine, T. Classification and Nomenclature of Somatostatin Receptors. *Trends Pharmacol. Sci.* **1995**, *16*, 86–88.
- (5) For a review of subtype-selective ligands, see refs 9–17 in: Rivier, J. E.; Hoeger, C.; Ercegyi, J.; Gulyas, J.; DeBoard, R.; Craig, A. G.; Koerber, S. C.; Wenger, S.; Waser, B.; Schaer, J.-C.; Reubi, J. C. Potent Somatostatin Undecapeptide Agonists Selective for Somatostatin Receptor 1 (sst1). *J. Med. Chem.* **2001**, *44*, 2238–2246.
- (6) Unpublished results from these laboratories.
- (7) The SARs of **2** at the NK1 and SRIF receptors illustrate the role of radial symmetry in the glucoside scaffold.^{8,9} Compound **2** binds not only the SRIF receptor for which it was designed, but also the NK1 and β_2 adrenergic receptors. These activities were discovered by serendipity, without systematic screening; furthermore, a close analogue of **2** blocks the interaction of I κ B with its kinase. [The authors are indebted to Dr. Carl DeCicco, Bristol-Myers Squibb Co. (formerly DuPont Pharmaceutical Company) for this information.] We have attributed this promiscuity to the radial symmetry of the glucose scaffold which is exemplified by the fact that **2** binds the sst4 and the NK1 receptors via side chains in positions 1,6 and 1,2, respectively. Cyclic hexapeptides, however, which lack such symmetry, bind both receptors via side chains in the $+1$ and $+2$ positions.^{8,9} It is important to appreciate that this promiscuity can be overcome because, although **2** binds diverse receptors, excellent specificity can be incorporated.
- (8) Liu, J.; Underwood, D. J.; Cascieri, M. A.; Rohrer, S. P.; Cantin, L.-D.; Chicchi, G.; Smith, A. B., III; Hirschmann, R. Synthesis of a Substance P Antagonist with a Somatostatin Scaffold: Factors Affecting Agonism/Antagonism at GPCRs and the Role of Pseudosymmetry. *J. Med. Chem.* **2000**, *43*, 3827–3831.
- (9) McVaugh, C. T.; Han, G.; Chicchi, G. G.; Underwood, D. J.; Prasad, V.; Liu, J.; Kurtz, M. M.; Birzin, E. T.; Cascieri, M. A.; Rohrer, S. P.; Smith, A. B., III; Hirschmann, R. Manuscript in preparation.
- (10) Fersht, A. R. The Hydrogen Bond in Molecular Recognition. *Trends Biochem. Sci.* **1987**, *12*, 301–304. (b) Fersht, A. R.; Shi, J.-P.; Knill-Jones, J.; Lowe, D. M.; Wilkinson, A. J.; Blow, D. M.; Brick, P.; Carter, P.; Waye, M. M. Y.; Winter, G. Hydrogen Bonding and Biological Specificity Analysed by Protein Engineering. *Nature* **1985**, *314*, 235–238.
- (11) Hunter, C. A.; Sanders, J. K. M. The Nature of π - π Interactions. *J. Am. Chem. Soc.* **1990**, *112*, 5252–5253.
- (12) Although it has been stated that the imidazol-4-ylmethyl and the pyridyl rings are bioisosteric,¹³ molecular modeling using the MM2* force field [Barbosa, J. (of these laboratories), private communication.] revealed poor overlap of the ring nitrogens of the imidazole in (+)-**13** with that of the pyridin-3-ylmethyl analogue (+)-**8**.
- (13) Robertson, D. W.; Krushinski, J. H.; Pollock, G. D.; Hayes, J. S. Imidazole-Pyridine Bioisosterism: Comparison of the Inotropic Activities of Pyridine and Imidazole-Substituted 6-Phenyldihydropyridazinone Cardiotonics. *J. Med. Chem.* **1988**, *31*, 461–465.
- (14) Berthelot, M.; Laurence, C.; Mohamed, S.; Besseau, F. Hydrogen-bond Basicity pK_{HB} Scale of Six-membered Aromatic N-Heterocycles. *J. Chem. Soc., Perkin Trans. 2* **1998**, 283–290. The pK_{HB} values are defined as the negative log of the equilibrium constants for hydrogen bond formation of the base of the heterocycle with 4-fluorophenol in CCl_4 , thus measuring H-bonding strengths directly.
- (15) Caminati, W.; Favero, L. B.; Favero, P. G.; Maris, A.; Melandri, S. Intermolecular Hydrogen Bonding Between Water and Pyrazine. *Angew. Chem., Int. Ed. Engl.* **1998**, *37*, 792–795.
- (16) The data suggest the possibility, but do not demonstrate, that both of the pyrazinyl nitrogen atoms are involved in hydrogen bonding.
- (17) Bone, R.; Agard, D. A. Mutational Remodeling of Enzyme Specificity. In *Methods in Enzymology*; Langone, J. J., Ed.; Acad. Press: New York, 1991; Chapter 28, Vol. 202, pp 643–670.
- (18) Steiner, T.; Koellner, G. Hydrogen Bonds with π -Acceptors in Proteins: Frequencies and Role in Stabilizing Local 3D Structures. *J. Mol. Biol.* **2001**, *305*, 535–557.
- (19) The modest affinity enhancement is not unexpected since on receptor binding the pyridine nitrogen's hydrogen bond with solvent is merely replaced by a hydrogen bond with the receptor.
- (20) Dunitz, J. D.; Taylor, R. Organic Fluorine Hardly Ever Accepts Hydrogen Bonds. *Chem.-Eur. J.* **1997**, *3*, 89–98.
- (21) See also the work of: (a) Murray-Rust, P.; Stallings, W. C.; Monti, C. T.; Preston, R. K.; Glusker, J. P. Intermolecular Interactions of the C–F Bond: The Crystallographic Environment of Fluorinated Carboxylic Acids and Related Structures. *J. Am. Chem. Soc.* **1983**, *105*, 3206–3214. (b) Shimoni, L.; Glusker, J. P. The Geometry of Intermolecular Interactions in Some Crystalline Fluorine-Containing Organic Compounds. *Struct. Chem.* **1994**, *5*, 383–397. (c) Howard, J. A. K.; Hoy, V. J.; O'Hagan, D.; Smith, G. T. How Good is Fluorine as a Hydrogen Bond Acceptor? *Tetrahedron* **1996**, *52*, 12613–12622.
- (22) O'Neill, B. M.; Ratto, J. E.; Good, K. L.; Tahmassebi, D. C.; Helquist, S. A.; Morales, J. C.; Kool, E. T. A Highly Effective Nonpolar Isostere of Deoxyguanosine: Synthesis, Structure, Stacking, and Base Pairing. *J. Org. Chem.* **2002**, *67*, 5869–5875 and references therein.
- (23) Rozovsky, S.; Jogl, G.; Tong, L.; McDermott, A. E. Solution-state NMR Investigations of Triosephosphate Isomerase Active Site Loop Motion: Ligand Release in Relation to Active Site Loop Dynamics. *J. Mol. Biol.* **2001**, *310*, 271–280.
- (24) See also: (a) Plenio, H.; Diodone, R. On the Protonation of Fluoro Cryptands and the Possibility of $CF\cdots HN^+$ Hydrogen Bonds. *Chem. Ber.* **1997**, *130*, 633–640. (b) Nangia, A. Packing Similarities in Organic Crystals with C–H/C–F Exchange. A Database Analysis of CH_3/CF_3 Pairs. *New J. Chem.* **2000**, *24*, 1049–1055. (c) Xiao, G.; Parsons, J. F.; Tesh, K.; Armstrong, R. N.; Gilliland, G. L. Conformational Changes in the Crystal Structure of Rat Glutathione Transferase M1–1 with Global Substitution of 3-Fluorotyrosine for Tyrosine. *J. Mol. Biol.* **1998**, *281*, 323–339.
- (25) Barberich, T. J.; Rithner, C. D.; Miller, S. M.; Anderson, O. P.; Strauss, S. H. Significant Inter- and Intramolecular O–H \cdots FC Hydrogen Bonding. *J. Am. Chem. Soc.* **1999**, *121*, 4280–4281.
- (26) Krueger, P. J.; Mettee, H. D. Spectroscopic Studies of Alcohols. I. Methanol-base Adducts in Dilute CCl_4 Solution. *Can. J. Chem.* **1964**, *42*, 288–293.
- (27) For other singular examples of fluorine acting as a H-bond acceptor, see: (a) Batsanov, A. S.; Collings, J. C.; Howard, J. A. K.; Marder, T. B. Octafluoronaphthalene-1,8-diaminonaphthalene (1/1). *Acta Crystallogr., Sect. E* **2001**, *E57*, 950–952. (b) Dubowchik, G. M.; Vrudhula, V. M.; Dasgupta, B.; Ditta, J.; Chen, T.; Sheriff, S.; Sipman, K.; Witmer, M.; Tredup, J.; Vyas, D. M.; Verdoorn, T. A.; Bollini, S.; Vinitzky, A. 2-Aryl-2,2-difluoroacetamide FKBP12 Ligands: Synthesis and X-ray Structural Studies. *Org. Lett.* **2001**, *3*, 3987–3990. (c) Takemura, H.; Kon, N.; Yasutake, M.; Nakashima, S.; Shinmyozu, T.; Inazu, T. The C–F \cdots Cation Interaction: An Ammonium Complex of a Hexafluoro Macrocyclic Cage Compound. *Chem.-Eur. J.* **2000**, *6*, 2334–2337.
- (28) Kim, C.-Y.; Chang, J. S.; Doyon, J. B.; Baird, T. T., Jr.; Fierke, C. A.; Jain, A.; Christianson, D. W. Contribution of Fluorine to Protein–Ligand Affinity in the Binding of Fluoroaromatic Inhibitors to Carbonic Anhydrase II. *J. Am. Chem. Soc.* **2000**, *122*, 12125–12134.
- (29) Atoji, M.; Lipscomb, W. N. The Crystal Structure of Hydrogen Fluoride. *Acta Crystallogr.* **1954**, *7*, 173–175. (b) Pauling, L. *The Nature of the Chemical Bond*, 3rd ed.; Cornell University Press: Ithaca, NY, 1960; pp 459–464.
- (30) Takahashi, L. H.; Radhakrishnan, R.; Rosenfield, R. E. Jr.; Meyer, E. F. Jr.; Trainor, D. A. Crystal Structure of the Covalent Complex Formed by a Peptidyl α,α -difluoro- β -keto Amide with Porcine Pancreatic Elastase at 1.78 Å Resolution. *J. Am. Chem. Soc.* **1989**, *111*, 3368–3374.
- (31) Brady, K.; Wei, A.; Ringe, D.; Abeles, R. H. Structure of Chymotrypsin-trifluoromethyl Ketone Inhibitor Complexes: Comparison of Slowly and Rapidly Equilibrating Inhibitors. *Biochemistry* **1990**, *29*, 7600–7607.
- (32) Wei, K.-T.; Ward, D. L. The Crystal and Molecular Structures of Ammonium Fluoroacetate, $C_2H_6FNO_2$, and Ammonium Difluoroacetate, $C_2H_5F_2NO_2$. *Acta Crystallogr., Sect. B* **1976**, *32*, 2768–2773.
- (33) Underwood, D. J., Bristol-Myers Squibb Co. (formerly DuPont Pharmaceutical Company), unpublished results.
- (34) Bauer, W.; Briner, U.; Doepfner, W.; Haller, R.; Huguenin, R.; Marbach, P.; Petcher, T.; Pless, J. SMS 201–995: A Very Potent and Selective Octapeptide Analogue of Somatostatin with Prolonged Action. *Life Sci.* **1982**, *31*, 1133–1140. (b) Pohl, E.; Heine, A.; Sheldrick, G. M.; Dauter, Z.; Wilson, K. S.; Kallen, J.; Huber, W.; Pfäffli, P. J. Structure of Octreotide, a Somatostatin Analogue. *Acta Crystallogr., Sect. D* **1995**, *51*, 48–59 and references therein. (c) Melacini, G.; Zhu, Q.; Goodman, M. Multiconformational NMR Analysis of Sandostatin (Octreotide): Equilibrium between β -Sheet and Partially Helical Structures. *Biochemistry* **1997**, *36*, 1233–1241.
- (35) Nutt, R., Merck Research Laboratories, private communication.
- (36) Veber, D. F.; Holly, F. W.; Paleveda, W. J.; Nutt, R. F.; Bergstrand, S. J.; Torchiana, M.; Glitzer, M. S.; Saperstein, R.; Hirschmann, R. Conformationally Restricted Bicyclic Analogues of Somatostatin. *Proc. Natl. Acad. Sci. U.S.A.* **1978**, *75*, 2636–2640.
- (37) The relationship between the C4 substituent of the sugar and Phe¹¹ is further complicated by the herringbone interactions between the side chains of Phe⁶ and Phe¹¹ of SRIF.

- (38) Burley, S. K.; Petsko, G. A. Aromatic-Aromatic Interaction: A Mechanism of Protein Structure Stabilization. *Science* **1985**, *229*, 23–28.
- (39) Depending on the polarization of the aromatic rings, the interaction can either be stabilizing or destabilizing. See: Hunter, C. A.; Lawson, K. R.; Perkins, J.; Urch, C. J. Aromatic Interactions. *J. Chem. Soc., Perkin Trans. 2* **2001**, 651–669. The extent of the contributions from the quadrupole moments of an aromatic system in stabilizing π -stacking interactions has been debated. Consensus holds that the role of quadrupole moments depends on the systems examined.
- (40) Some authors have suggested that there is a significant 'through-space' polar/ π interaction.^{41,42} Others suggest that the electrostatic potential of aromatic systems do not significantly affect aryl-aryl interactions. See: Kim, E.-I.; Paliwal, S.; Wilcox, C. S. Measurements of Molecular Electrostatic Field Effects in Edge-to-Face Aromatic Interactions and CH- π Interactions with Implications for Protein Folding and Molecular Recognition. *J. Am. Chem. Soc.* **1998**, *120*, 11192–11193; Gellman, S. H.; Haque, T. S.; Newcomb, L. F. New Evidence that the Hydrophobic Effect and Dispersion are not Major Driving Forces or Nucleotide Base Stacking. Comments. *Biophys. J.* **1996**, *71*, 3523–3526.
- (41) Cozzi, F.; Cinquini, M.; Annunziata, R.; Dwyer, T.; Siegel, J. S. Polar/ π Interactions between Stacked Aryls in 1,8-Diarylnaphthalenes. *J. Am. Chem. Soc.* **1992**, *114*, 5729–5733.
- (42) Doyon, J. B.; Jain, A. The Pattern of Fluorine Substitution Affects Binding Affinity in a Small Library of Fluoroaromatic Inhibitors for Carbonic Anhydrase. *Org. Lett.* **1999**, *1*, 183–185.
- (43) Samanta, U.; Chakrabarti, P.; Chandrasekhar, J. Ab Initio Study of Energetics of X-H $\cdots\pi$ (X = N, O, and C) Interactions Involving a Heteroatomic Ring. *J. Phys. Chem. A* **1998**, *102*, 8964–8969.
- (44) (a) MacSpartan Pro/Macspartan Plus (version 2.0) User's Guide, Wave function: Irvine, CA, 2000; pp 64–69. (b) Hehre, W. J.; Yu, J.; Klunzinger, P. E.; Lou, L. A Brief Guide to Molecular Mechanics and Quantum Chemical Calculations. Wave function: Irvine, CA, 1998; pp 138–139. (c) Thornton, E. R. University of Pennsylvania. Unpublished results.
- (45) Kaupmann, K.; Bruns, C.; Raulf, F.; Weber, H. P.; Mattes, H.; Lubbert, H. Two Amino Acids, Located in Transmembrane Domains VI and VII, Determine the Selectivity of the Peptide Agonist SMS 201–995 for the SSTR2 Somatostatin Receptor. *EMBO J.* **1995**, *14*, 727–735.
- (46) Nutt, R. F.; Veber, D. F. Merck Research Laboratories, private communication.
- (47) Veber, D. F.; Strachan, R. G.; Bergstrand, S. J.; Holly, F. W.; Homnick, C. F.; Hirschmann, R.; Torchiana, M. L.; Saperstein, R. Nonreducible Cyclic Analogues of Somatostatin. *J. Am. Chem. Soc.* **1976**, *98*, 2367–2369.
- (48) Prasad, V. Ph.D. Thesis, University of Pennsylvania, 2001.
- (49) Pigman, W. W. Specificity, Classification, and Mechanism of Action of the Glycosidases. In *Advances in Enzymology*; Nord, F. F., Werkman, C. H., Eds.; Interscience: New York, 1946; Vol. 4, pp 41–65. (b) Fischer, E. Einfluss der Configuration auf die Wirkung der Enzyme. *Chem. Ber.* **1894**, *27*, 2985–2993.
- (50) Capon, B. Mechanism in Carbohydrate Chemistry. *Chem. Rev.* **1969**, *69*, 415–426 and references therein.
- (51) Fujita, T.; Iwasa, J.; Hansch, C. A New Substituent Constant, π , Derived from Partition Coefficients. *J. Am. Chem. Soc.* **1964**, *86*, 5175–5180. (b) Hansch, C.; Maloney, P. P.; Fujita, T.; Muir, R. M. Correlation of Biological Activity of Phenoxyacetic Acids with Hammett Substituent Constants and Partition Coefficients. *Nature (London)* **1962**, *194*, 178–180.
- (52) Dorsey, B. D.; McDonough, C.; McDaniel, S. L.; Levin, R. B.; Newton, C. L.; Hoffman, J. M.; Darke, P. L.; Zugay-Murphy, J. A.; Emini, E. A.; Schleif, W. A.; Olsen, D. B.; Stahlhut, M. W.; Rutkowski, C. A.; Kuo, L. C.; Lin, J. H.; Chen, I.-W.; Michelson, S. R.; Holloway, M. K.; Huff, J. R.; Vacca, J. P. Identification of MK-944a: A Second Clinical Candidate from the Hydroxylaminepentanamide Isostere Series of HIV Protease Inhibitors. *J. Med. Chem.* **2000**, *43*, 3386–3399.
- (53) Prasad, V., et al., manuscript in preparation.
- (54) Chan, O. H.; Stewart, B. H. Physicochemical and Drug-delivery Considerations for Oral Drug Bioavailability. *Drug Discovery Today* **1996**, *1*, 461–473.
- (55) Musser, J. H.; Fugedi, P.; Anderson, M. B. Carbohydrate Therapeutics. In *Burger's Medicinal Chemistry and Drug Discovery*; Wolff, M. E., Ed.; John Wiley & Sons: New York, 1995; Vol. 1, p 902.
- (56) Huber, G.; Rossi, A. Etherified carbohydrates. I. Tribenzyl-D-glucofuranosides, a new group of medicinal carbohydrates. *Helv. Chim. Acta* **1968**, *51*, 1185–1202.
- (57) Previously reported in ref 2.
- (58) Hirschberg, A.; Spoerri, P. E. Chlorination of Some Alkylpyrazines. *J. Org. Chem.* **1961**, *26*, 2356–2360.; (b) Abushanab, E.; Bindra, A. P.; Goodman, L.; Peterson, H., Jr. Imidazo[1,5-*a*]pyrazine System. *J. Org. Chem.* **1973**, *38*, 2049–2052. (c) Newkome, G. R.; Kiefer, G. E.; Xia, Y.-J.; Gupta, V. K. Chemistry of Heterocyclic Compounds. Part 74. α -Methyl Functionalization of Electron-poor Heterocycles: Free Radical Chlorination. *Synthesis* **1984**, 676–679.
- (59) Staudinger, H.; Meyer, J. New Organic Compounds of Phosphorus. III. Phosphinemethylene Derivatives and Phosphinimines. *Helv. Chim. Acta* **1919**, *2*, 635–646.
- (60) Scriven, E. F. V.; Turnbull, K. Azides: Their Preparation and Synthetic Uses. *Chem. Rev.* **1988**, *88*, 297–368. (b) Gololobov, Y. G.; Zhmurova, I. N.; Kasukhin, L. F. Sixty Years of Staudinger Reaction. *Tetrahedron* **1981**, *37*, 437–472.
- (61) Hynes, J. J., Ph.D. Thesis, University of Pennsylvania, 1996.
- (62) (a) Staros, J. V.; Bayley, H.; Standring, D. N.; Knowles, J. R. Reduction of Aryl Azides by Thiols: Implications for the Use of Photoaffinity Reagents. *Biochem. Biophys. Res. Commun.* **1978**, *80*, 568–572. (b) Bayley, H.; Standring, D. N.; Knowles, J. R. Propane-1,3-dithiol: A Selective Reagent for the Efficient Reduction of Alkyl and Aryl Azides to Amines. *Tetrahedron Lett.* **1978**, *19*, 3633–3634.
- (63) Nilsson, M.; Svahn, C.-M.; Westman, J. Synthesis of the Methyl Glycosides of a Tri- and a Tetra-saccharide Related to Heparin and Heparan Sulphate. *Carbohydrate Res.* **1993**, *246*, 161–172.
- (64) Birzin, E. T.; Rohrer, S. P. High-throughput Receptor-binding Methods for Somatostatin Receptor 2. *Anal. Biochem.* **2002**, *159*–166.
- (65) Harris, D. C. Statistics. In *Quantitative Chemical Analysis*, 3rd ed.; W. H. Freeman: New York, 1991; Chapter 4, pp 47–63.

JM0205088